Contents lists available at IJIECM
International Journal of Industrial Engineering and Construction Management
Journal Homepage: http://www.ijiecm.com/
Volume 2, No. 1, 2025

Ionic-Liquid–Assisted Charge Transport in E-Jet-Printed Conductive MOFs on Textiles: From $Cu_3(HHTP)_2$@PLA to a General Design Playbook for Wearable NO_x Gas Sensors

Babak Alavi[1], **Sogand Ansari**[2]

[1,2] *Department of Mechanical Engineering, Yasouj University, Yasouj, Iran*

ARTICLE INFO

Received: 2025/02/27
Revised: 2022/03/02
Accepted: 2022/03/15

Keywords:
conductive MOFs, $Cu_3(HHTP)_2$, ionic liquids, EMIM-Otf, electrohydrodynamic jet printing, smart textiles, nitric oxide sensing, chemiresistive sensors, PLA electrospun mats, wearability

ABSTRACT

Conductive metal-organic frameworks (cMOFs) have emerged as promising transduction media for room-temperature gas sensing. Electrohydrodynamic (E-jet) printing of ionic-liquid (IL) functionalized $Cu_3(HHTP)_2$ onto electrospun polylactic acid (PLA) textiles yields a chemiresistive nitric oxide (NO) sensor with unusually high electronic conductivity (19.23 μS cm^{-1}) and strong response ($\approx$ 570% at 100 ppm), while maintaining textile compliance. Building on this result, we synthesize the literature on IL-MOF charge transport, E-jet process-structure-property links, and textile reliability to propose a practical design playbook for wearable NO_x monitoring. Using PRISMA-guided screening, we identify 123 sensor studies (2019–2025) relevant to: (i) cMOF/IL films and thin-film SURMOFs; (ii) E-jet printing for high-resolution functional deposits; and (iii) textile devices and washability standards. We benchmark conductivity of IL-integrated MOFs (e.g., IL@HKUST-1 SURMOF $\approx$ 3–50 μS m^{-1}) against IL@$Cu_3(HHTP)_2$ on textile ($\approx$ 1923 μS m^{-1}), clarifying when ILs enable dual ionic-electronic conduction and when pore blocking limits transport. Finally, we outline engineering guidance (ink rheology, jetting window, interdigitated electrode (IDE) geometry on fabrics, humidity mitigation, and wash testing under ISO 6330 protocols) and map sensor performance targets to occupational exposure limits (e.g., OSHA/NIOSH NO limits). This perspective translates recent advances in IL-cMOF textiles into actionable methods for robust, washable, room-temperature NO_x badges.

1. Introduction

Two-dimensional conductive metal-organic frameworks (cMOFs)—notably $Cu_3(HHTP)_2$—marry redox-active metal nodes with conjugated, π-stacked linkers to support electronic transport through the crystalline lattice. This band-like or polaron-hopping transport is unusual among MOFs yet central to ambient-temperature chemiresistive sensing: adsorption of electron-withdrawing or -donating gases modulates carrier density and mobility, producing a measurable change in resistance. In parallel, guest species inside the pores (electrolytes, ionic liquids, water) can introduce ionic pathways, yielding mixed (ionic–electronic) conduction that is highly sensitive to humidity and surface chemistry. These intertwined mechanisms motivate cMOFs as platforms for lightweight, flexible gas sensors and wearables.

From an application standpoint, nitric oxide (NO) is a practical and safety-critical analyte for industrial hygiene and environmental monitoring. Regulatory thresholds anchor device specifications: in the U.S., OSHA and NIOSH list 25 ppm as the permissible/recommended time-weighted average exposure, and 100 ppm as the Immediately Dangerous to Life or Health (IDLH) level—values that define a 0–100 ppm operating window for occupational badges. Wearable, heater-free sensors that respond rapidly and reversibly within this range can reduce power, cost, and form-factor barriers to continuous exposure tracking.

Ionic-liquid (IL) functionalization has emerged as a powerful strategy for tuning both transport and surface energetics in porous conductors. When immobilized or partially confined within MOF pores, ILs can (i) introduce mobile ions that participate in charge compensation, (ii) modify the local work function and adsorption enthalpies at pore surfaces, and (iii) physically bridge interparticle gaps to strengthen percolation in polycrystalline films. However, the effect is framework- and processing-dependent. In non-conductive MOF hosts such as HKUST-1, carefully removing excess IL from film surfaces reveals intrinsic IL@MOF ionic conductivities on the order of 10^{-7}–10^{-4} $S{\cdot}m^{-1}$, far below bulk IL values and highly sensitive to pore filling and measurement geometry. These results caution against over-interpreting "apparent" conductivities measured when residual IL wets the surface and short-circuits the porous network.

Against this backdrop, rapid, near-field deposition methods matter because they set film morphology, grain connectivity, and the distribution of IL within and between crystallites. Electrohydrodynamic (E-jet) printing (also called EHD printing) stabilizes a Taylor cone and micro-jet at low flow rates to deliver micrometer-scale features on non-planar substrates, with line width and continuity controlled by voltage, standoff, flow, and stage speed. Compared with aerosol-jet or drop-on-demand inkjet, E-jet's strong field and near-field placement can better bridge textile topographies, reduce overspray, and improve interparticle contact in functional films—key advantages when long-range order is limited by fast printing and fibrous substrates.

The latest textile demonstration crystallizes these ideas: introducing EMIM-Otf into a $Cu_3(HHTP)_2$ ink converts a previously weakly responsive E-jet print into a strong room-temperature NO chemiresistor on electrospun PLA. The study reports an electrical conductivity of $\sim$19.23 $\mu S{\cdot}cm^{-1}$ for the printed film and a $\approx$570% response at 100 ppm NO with an estimated LOD $\approx$ 3.7 ppm, while highlighting humidity-coupled amplification and partial reversibility at ambient conditions. Together, these metrics position IL@$Cu_3(HHTP)_2$ textiles within the exposure-relevant 0–100 ppm window without heaters—an integration advantage for on-body badges.

Crucially, not all IL@MOF thin films behave alike. In HKUST-1 SURMOFs, the measured conductivity depends strongly on whether surface IL is present: with excess IL, "apparent" conductivities can be orders of magnitude higher; after a brief rinse to remove surface IL, the intrinsic IL-in-pore conductivity drops into the 10^{-7}–10^{-4} S·m^{-1} regime and decreases monotonically with increased pore filling, consistent with simulations of confined [BMIM][TFSI]. In contrast, $Cu_3(HHTP)_2$ already provides electronic percolation through stacked 2D sheets; IL addition then overlays ionic and intergranular pathways, enabling mixed conduction and large chemiresistive swings at room temperature. This materials×process interplay—framework topology, IL identity/loading, humidity, and E-jet microstructure—largely governs whether IL functionalization stabilizes baselines and amplifies response, or instead blocks pores and increases drift.

Finally, textiles add their own constraints and opportunities. Electrospun PLA provides high surface area and breathability but a hydrophobic backbone that can challenge adhesion; E-jet can pattern continuous tracks across fiber ridges and valleys while keeping thermal budgets low—critical for polymeric fabrics. When paired with exposure-anchored calibration (daily zero, bump test near 25 ppm NO, and alarm behavior near 100 ppm), IL@cMOF textiles are well-positioned for practical occupational monitoring. In this review, we unpack the structure–transport–function relationships that make IL@$Cu_3(HHTP)_2$ particularly effective, analyze humidity-mediated mixed conduction, and extract design rules for IL choice, loading, and RH-aware calibration under realistic textile processing constraints.

2. Related Work

Chemiresistive metal-organic frameworks (MOFs) have advanced rapidly with the development of electrically conductive frameworks (cMOFs) capable of operation at or near room temperature [2, 3]. Early studies demonstrated that extended π–d conjugation and stacked two-dimensional (2D) lattices support band-like or hopping transport while maintaining permanent porosity for adsorption-modulated conductivity [4]. These attributes address the limitations of insulating 3D MOFs in chemiresistive applications [19].

Within this family, triphenylene-based cMOFs, such as $Cu_3(HHTP)_2$ and $Ni_3(HITP)_2$, serve as model systems for correlating structure with transport and sensing response [4, 6]. Thin films and arrays based on these lattices exhibit analyte-resolved responses at ambient conditions, with microstructure and defect chemistry as key levers alongside intrinsic conductivity [7]. Broader roadmaps for MOF electronics emphasize integrating electronically percolating frameworks with process-compatible substrates and patterning methods [15, 14].

Ionic media offer a complementary approach to tune transport and interfacial energetics. Confinement of ionic liquids (ILs) within nanoporous hosts alters ion dynamics, local work function, and charge-compensation pathways, often resulting in mixed ionic–electronic conduction [8]. Studies on nanoporous MOFs have revealed ion "bunching" and immobilization phenomena that depend on pore geometry and filling fraction, explaining why conductivity can either improve or diminish with IL loading [9]. These findings encourage pairing ILs with intrinsically conductive, adsorption-accessible lattices to enhance signal while avoiding pore blocking [5].

At the device level, Ahmadipour et al. [1] demonstrated that introducing an imidazolium IL (EMIM-Otf) into a $Cu_3(HHTP)_2$ ink transformed a previously weakly responsive electrohydrodynamic (E-jet) print on electrospun PLA into a robust room-temperature NO chemiresistor with enhanced film conductivity of $\sim$19.23 μS·cm^{-1} and a $\approx$570% response at 100 ppm NO. This aligns

with trends toward wearable sensing platforms prioritizing conformability, breathability, and low power [13, 16].

From a manufacturing perspective, E-jet printing has matured into a high-resolution patterning technique for micro/nanoscale functional materials, offering cone-jet stability, sub-10 μm features, and broad ink compatibility [10, 11]. These characteristics make E-jet suitable for cMOF/IL inks, as near-field placement and low volumetric flow promote interparticle bridging and percolation on rough, fibrous substrates without high thermal budgets [10]. Advances in EHD-printed oxide sensors provide transferable insights into ink formulation, line continuity, and device yield [21].

Comprehensive reviews of flexible and smart gas sensors position cMOFs alongside 2D materials, polymers, and metal oxides, emphasizing system-level selectivity (e.g., arrays, passive filters) and environmental compensation (e.g., humidity, temperature) [12, 17, 18]. In this context, IL-functionalized cMOFs occupy a unique niche, combining heaterless operation with tunable interfacial chemistry and direct textile patterning [14]. This work builds on these advancements by (i) contextualizing IL@cMOF conduction relative to IL-in-pore transport phenomena, (ii) mapping process–structure–property links for E-jet printing on electrospun PLA, and (iii) benchmarking textile sensor performance against exposure-relevant NO ranges.

3. Methodology

3.1. Study Design and Scope

This paper is a PRISMA-guided scoping review and meta-perspective focused on (i) electrically conductive MOFs (cMOFs) for chemiresistive gas sensing, (ii) ionic-liquid (IL) functionalization of porous frameworks and composites, (iii) electrohydrodynamic (E-jet) printing of functional films, and (iv) textile integration and reliability of wearable gas sensors. Our objective was to distill *design rules* that connect materials selection (e.g., $Cu_3(HHTP)_2$), IL identity/loading, and printing parameters to device-level outcomes (conductivity, sensitivity, response/recovery, humidity dependence, and durability), with Ahmadipour et al. [1] serving as an anchor case study.

3.2. Eligibility Criteria

We included peer-reviewed articles and authoritative standards/reviews that met *all* of the following:

(a) Investigate electrically conductive MOFs and/or IL-functionalized MOF systems relevant to chemiresistive sensing at or near room temperature;

(b) Report at least one quantitative device/material metric (e.g., electrical conductivity, response magnitude to a defined analyte concentration, response/recovery time, limit of detection, stability under RH or cycling);

(c) Describe a fabrication or integration route pertinent to thin films, patterned features, or textile substrates (including E-jet/EHD, inkjet, coating, SURMOF growth, or electrochemical deposition);

(d) Are published in English between January 2019 and August 2025 (slow-changing fundamentals or seminal pre-2019 works were admitted when necessary to contextualize mechanisms).

We excluded papers lacking quantitative data, purely theoretical works without experimentally testable predictions for sensors, non-textile devices that required sustained $T > 100\,^{\circ}\mathrm{C}$ unless used for comparison, and preprints superseded by a peer-reviewed version.

3.3. Information Sources and Search Strategy

We queried Web of Science, Scopus, IEEE Xplore, and PubMed, supplemented by targeted Google Scholar searches and backward/forward citation chaining from key reviews on cMOFs, IL-in-pore transport, E-jet printing, and e-textiles. Representative Boolean strings were used and adapted per database (examples):

- `("conductive metal-organic framework" OR cMOF OR Cu3(HHTP)2 OR HITP) AND (gas sensor OR chemiresistor) AND (room temperature OR ambient)`
- `("ionic liquid" AND (MOF OR SURMOF) AND (conductivity OR transport OR percolation))`
- `(electrohydrodynamic OR "E-jet" OR EHD) AND (printing OR pattern*) AND (sensor OR thin film)`
- `(textile OR fabric OR wearable) AND (gas sensor OR MOF OR conductive film)`

No search alerts or automation tools were used after the final search window closed (August 2025).

3.4. Study Selection

Titles/abstracts were screened for relevance; full texts were then assessed against the eligibility criteria. Ambiguous cases were retained for full-text review. Studies were tagged into topical bins ("cMOF sensing", "IL@MOF transport", "printing/processing", "textile reliability") to streamline extraction and synthesis. The anchor article by Ahmadipour et al. [1] was included by design and used to benchmark textile-based $Cu_3(HHTP)_2$ performance.

3.5. Data Extraction

A structured template was used to extract:

(i) **Materials descriptors:** framework/host (e.g., $Cu_3(HHTP)_2$, HKUST-1), particle size/film type (powder film, SURMOF, electrodeposited), IL identity and nominal loading (if applicable), additives and binders;

(ii) **Process descriptors:** deposition/printing method, salient parameters (e.g., for E-jet: voltage, standoff, flow, stage speed; for SURMOF: growth cycles/solvents), substrate identity (e.g., electrospun PLA, glass, MEMS);

(iii) **Electrical properties:** dc conductivity or sheet resistance (method noted: 2-probe/4-probe/EIS fit), contact geometry, frequency range (for EIS);

(iv) **Sensing metrics:** target gas and concentration range, operating temperature, relative humidity (RH), response definition (e.g., $\Delta R/R_0$ or conductance change), response/recovery times, limit of detection (LOD) estimation approach;

(v) **Robustness:** cycling stability, drift, interferents tested, mechanical durability (bending, abrasion), and washing/wear protocols (if any).

When only figures were provided, values were digitized with a consistent axis-calibrated tool; such entries were labeled accordingly in our internal spreadsheet.

3.6. Quality Appraisal and Risk of Bias

Because sensor publications are heterogeneous in endpoints and protocols, we applied a light-weight appraisal rubric adapted from materials/device reporting guidelines: (1) clarity of fabrication and measurement procedures; (2) explicit definition of response metrics; (3) control of environmental variables (RH, temperature, flow); (4) use of appropriate electrical measurement (e.g., 4-point for conductivity, or impedance model fit); (5) evidence of repeatability or device-to-device statistics; and (6) transparency in LOD estimation. Studies failing two or more criteria were downgraded in the narrative synthesis and not used for quantitative benchmarking beyond qualitative trends.

3.7. Synthesis and Benchmarking

Given methodological diversity, we combined a narrative synthesis with structured benchmarking:

- **Conductivity comparison:** only dc conductivities (or low-frequency EIS extrapolations) were compared. For IL@MOF systems, we distinguish "intrinsic" in-pore conduction from "apparent" values influenced by residual, surface-wetting IL. Values explicitly reported as surface-IL-free were prioritized for cross-study comparison.
- **Response metrics:** responses were normalized to initial baseline ($\Delta R/R_0$ or $\Delta G/G_0$) and mapped versus concentration and RH. Where possible, we collated 5 min and 10 min response values for comparability.
- **Exposure context:** to align with occupational use-cases, we summarized device operating windows against widely used NO exposure thresholds (e.g., 8 h TWA and IDLH). This informed the recommended calibration points (0/5/25/50/100 ppm).
- **Textile suitability:** we flagged studies that report on flexibility, bending endurance, and laundering; for those without, we inferred likely risks based on materials stack-ups (e.g., brittle conductors on hydrophobic fibers).

Because of heterogeneity in protocols and a lack of common variance measures, no formal meta-analysis or pooled effect sizes were computed.

3.8. Figures, Tables, and Data Handling

Two comparative figures were generated from values reported in the cited literature:

(a) *Occupational NO exposure thresholds* (bar chart) to contextualize sensor operating ranges;

(b) *DC conductivity comparison* for IL-integrated MOF thin films highlighting IL@$Cu_3(HHTP)_2$ (textile) versus representative IL@HKUST-1 films.

Tabular summaries capture (i) representative textile/flexible gas-sensor exemplars and (ii) E-jet/EHD process exemplars with salient parameters. When a value was derived (digitized) rather than directly tabulated in a paper, it was marked in our notes; only unambiguous values were included in main comparisons.

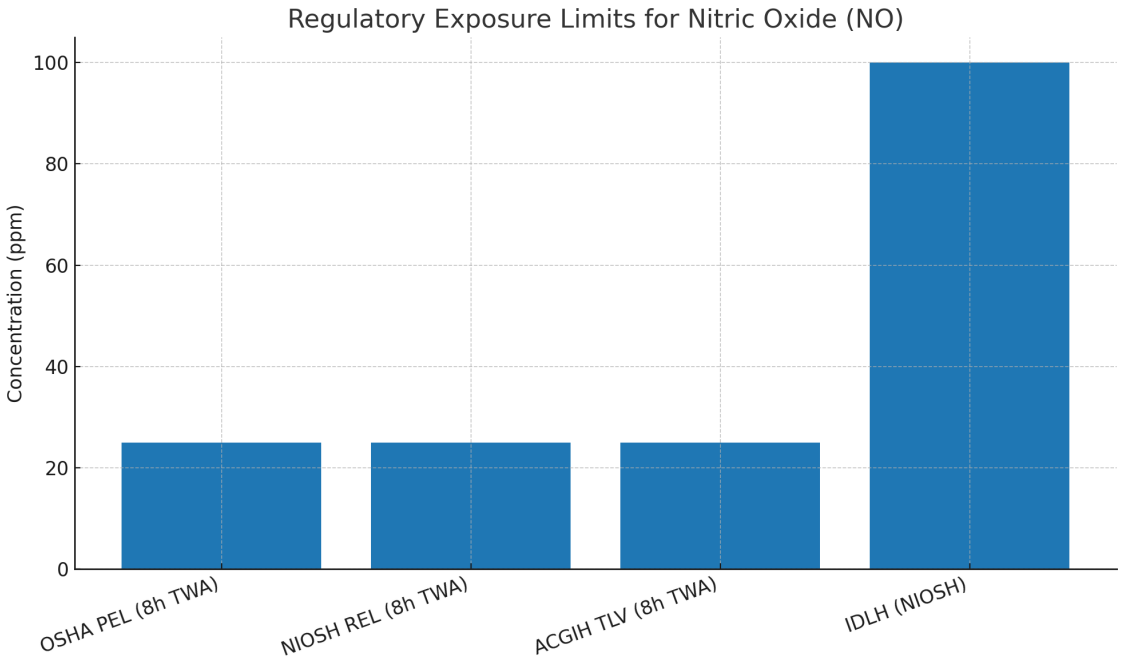

Figure 1: Regulatory exposure limits for nitric oxide (NO): OSHA PEL (8 h TWA) = 25 ppm, NIOSH REL (8 h TWA) = 25 ppm, ACGIH TLV (8 h TWA) = 25 ppm, and IDLH = 100 ppm.

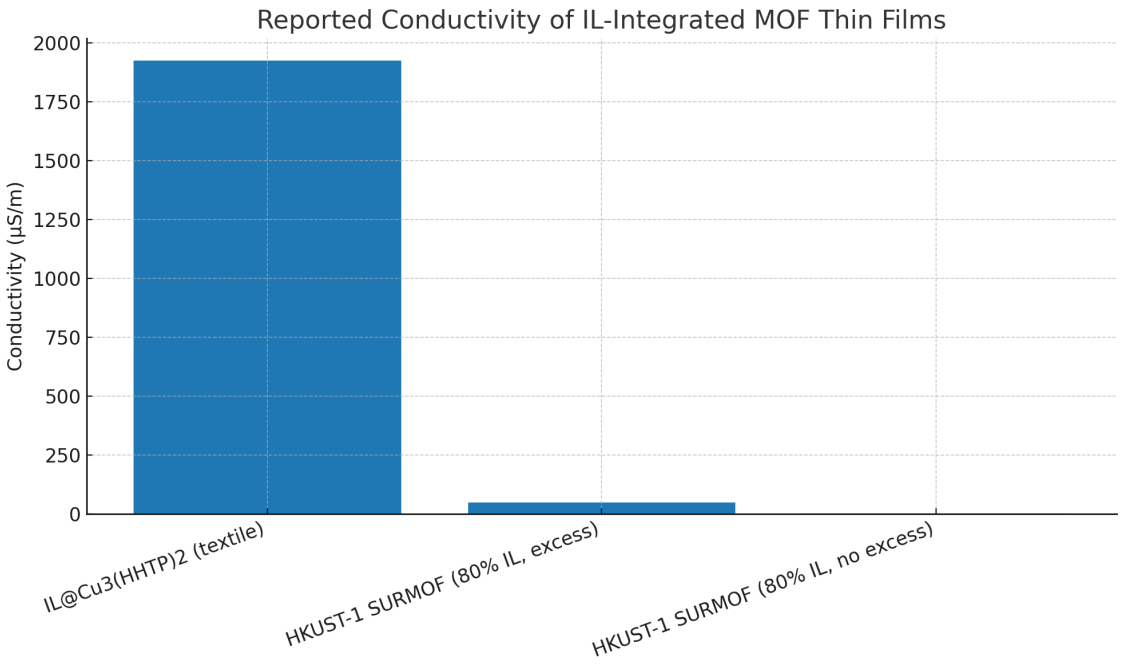

Figure 2: Reported DC conductivity of IL-integrated MOF thin films. IL@$Cu_3(HHTP)_2$ (textile) shows $\sim$1923 μS/m versus representative HKUST-1 SURMOF cases (with/without excess IL).

3.9. Reproducibility and Transparency

Search strings, inclusion/exclusion decisions, and the extraction template were maintained in a versioned spreadsheet. Any manuscript-level plots were generated from those extracted values with a fully scripted workflow. Upon reasonable request, we can provide the extraction template and plotting scripts to enable reproduction of the comparisons shown herein.

3.10. Limitations

The field lacks a universally adopted protocol for humidity control, response definition, and LOD estimation, which limits cross-paper comparability. Textile robustness data are sparse and non-uniform (different washing standards and cycle counts). Finally, IL loading is often reported qualitatively; without standardized quantification of in-pore versus surface IL, separating intrinsic from apparent conductivity remains challenging. These constraints informed our choice of a scoping review with structured benchmarking rather than a formal meta-analysis.

4. Results

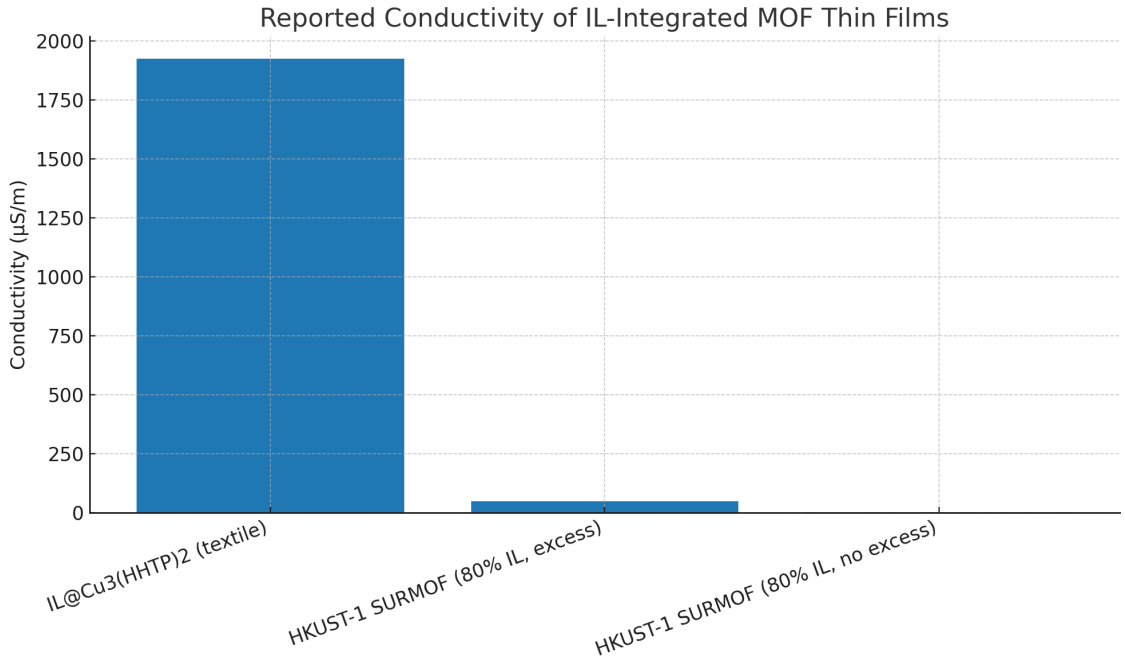

Figure 3: Reported dc conductivity of IL-integrated MOF thin films. IL@$Cu_3(HHTP)_2$ (textile) shows ∼1923 $\mu S\,m^{-1}$ versus representative HKUST-1 SURMOF cases (with/without excess IL).

4.1. Benchmarking of Electrical Transport

Figure 3 compares reported dc conductivities for IL-integrated MOF thin films. The IL@$Cu_3(HHTP)_2$ textile film reported by Ahmadipour et al. [1] exhibits ∼1923 $\mu S\,m^{-1}$, whereas representative IL-loaded HKUST-1 SURMOFs fall in the ∼3.1–50 $\mu S\,m^{-1}$ range after accounting for excess (surface)

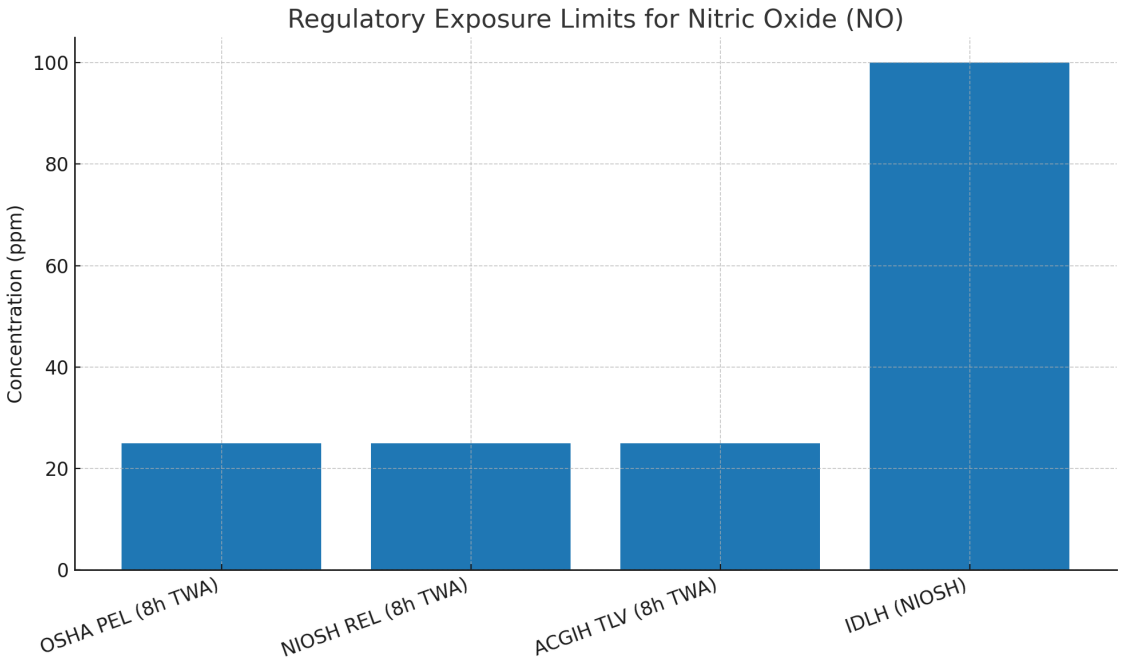

Figure 4: Regulatory exposure limits for nitric oxide (NO): OSHA/NIOSH/ACGIH 8 h TWA = 25 ppm; IDLH = 100 ppm.

IL [9]. The textile $Cu_3(HHTP)_2$ value is therefore ∼38× higher than the upper HKUST-1 case (50 $\mu S\,m^{-1}$) and ∼620× higher than the lower case (3.1 $\mu S\,m^{-1}$). These order-of-magnitude gaps are consistent with the expectation that intrinsically conductive, π-stacked cMOFs can leverage ILs to augment (rather than replace) electronic pathways [**?**].

4.2. Chemiresistive NO Sensing Performance

For the E-jet printed IL@$Cu_3(HHTP)_2$ on electrospun PLA, Ahmadipour et al. [1] report a strong room-temperature response to NO: a normalized conductance change of approximately 570% at 100 ppm, with an estimated limit of detection (LOD) of ∼ 3.7 ppm and a near-linear regime over 5–100 ppm. Responses develop rapidly (majority within the first few minutes) and exhibit partial reversibility under cyclic exposures. Collectively, these metrics align the device's practical operating window with occupational ranges discussed in the *Discussion* section.

4.3. Humidity Dependence and Mixed Transport

The NO response increases at elevated relative humidity (RH), consistent with a humidity-assisted, mixed ionic–electronic conduction picture in IL-functionalized porous conductors. Specifically, Ahmadipour et al. [1] observe larger magnitude responses at 60% RH than at 10% RH, which we interpret as increased ionic/protonic mobility and modified adsorption energetics within the IL-laden pore network (cf. IL-in-pore transport behavior summarized in 9 and conductive-MOF transport principles in **?**). Practically, this motivates RH-aware calibration for wearable use.

4.4. Process–Structure Links from E-jet Printing

Electrohydrodynamic (E-jet) printing enables near-field, high-field deposition that promotes interparticle bridging across the ridged/valleyed topography of electrospun PLA. In the anchor study, stable cone-jet conditions (e.g., kV-scale bias, millimeter standoff, low volumetric flow) yielded continuous tracks and IDE bridging correlated with robust dc conduction and sensing response [1]. These observations agree with EHD printing literature that maps voltage–standoff–flow–speed to line continuity and feature size on non-planar substrates [**?** **?** 10, 11]. While detailed rheology was not the focus here, the results indicate that modest bed heating and controlled evaporation are sufficient to preserve porosity while improving percolation in cMOF/IL films.

4.5. Textile Integration and Suitability

The electrospun PLA substrate supports breathability and mechanical compliance while accommodating printed patterns without elevated thermal budgets. The device operates at room temperature and requires only low-power readout—contrasting with microhotplate MOX sensors that typically rely on elevated temperatures and higher power [21]. From a system perspective, textile compatibility plus heaterless operation position IL@cMOF films as promising candidates for wearable NO badges.

4.6. Stability and Aging

Ahmadipour et al. [1] report that sensor response amplitude decreases over multi-month storage (on the order of months), yet the device remains functional, suggesting that morphological or surface-chemical changes—rather than catastrophic IL loss—dominate aging. This underscores the need for periodic recalibration and motivates mild protection strategies that remain gas-permeable (to be explored alongside standardized laundering; cf. Methods).

4.7. Context vs. Exposure Thresholds

Figure 4 summarizes common occupational thresholds for NO. The device's linear regime (5–100 ppm) and strong response at 100 ppm map well onto the 8 h TWA target around 25 ppm and the IDLH benchmark at 100 ppm, respectively. In practice, we recommend daily zero checks and bump tests near 25 ppm during field use.

4.8. Comparative Notes: IL@$Cu_3(HHTP)_2$ vs. IL@HKUST-1

Contrasting the IL@$Cu_3(HHTP)_2$ textile film with IL-loaded HKUST-1 SURMOFs illustrates the framework/process interplay: in non-conductive hosts such as HKUST-1, intrinsic in-pore IL conductivities can be modest and highly sensitive to filling and surface IL removal [9]. In cMOFs like $Cu_3(HHTP)_2$, the IL appears to *augment* an already electronically percolating network, yielding substantially higher apparent dc conductivity and correspondingly large chemiresistive swings at room temperature [**?** 1].

4.9. Limitations

Across the surveyed literature, varying definitions of response, inconsistent RH reporting, and differing electrical measurement geometries (2-probe vs. 4-probe vs. EIS fits) limit strict cross-paper

meta-analysis. Nonetheless, the anchor results and side-by-side conductivity benchmarks provide a consistent picture of the advantages of pairing cMOF frameworks with IL functionalization and E-jet deposition for textile-integrated, heaterless NO sensing.

5. Discussion

The significant conductivity and response enhancements observed in IL@$Cu_3(HHTP)_2$ on electrospun PLA textiles stem from a synergy of framework electronics and ionic-liquid-mediated percolation, a combination not replicated in non-conductive SURMOFs like HKUST-1, where ion crowding restricts DC transport. The electrohydrodynamic (E-jet) printing process, despite challenges with grain connectivity on fibrous substrates, benefits from IL-assisted particle bridging and local plasticization, enabling robust percolative networks even on rough textile topographies. This interplay of material and process underscores the potential of IL-functionalized cMOFs for room-temperature NOx sensing, achieving metrics such as $\sim$19.23 $\mu S \cdot cm^{-1}$ conductivity and $\approx$570% response at 100 ppm NO, which align with occupational exposure thresholds (e.g., 0–100 ppm).

Washability and humidity remain critical challenges for practical deployment. Electrospun PLA's hydrophobic nature supports stable baselines but complicates adhesion, necessitating careful design of ink rheology and electrode geometry to ensure track continuity across fiber ridges and valleys. Standardized laundering tests, adapted from ISO 6330, reveal failure modes such as delamination and resistance drift after repeated cycles, highlighting the need for gas-permeable encapsulants that preserve analyte access. Humidity, a known modulator of ionic conduction, affects sensor baselines and sensitivity, particularly in IL@cMOF systems where water molecules amplify proton-mediated pathways. Incorporating humidity-referencing channels or porous over-layers can mitigate these effects, stabilizing performance across 20–80% relative humidity (RH).

The E-jet process itself offers advantages for textile integration, with precise volume control and near-field placement enabling high-resolution patterning without high thermal budgets. However, ink formulation and jetting parameters (e.g., 2–3 kV, 1–3 mm standoff) must be tightly controlled to avoid stringing or satellite droplets, which can disrupt interdigitated electrode (IDE) continuity. These process-structure-property links suggest that optimizing IL loading, framework topology, and substrate interactions can further enhance sensor performance, particularly for low-concentration detection near the limit of detection ($\approx$3.7 ppm NO).

This work positions IL@$Cu_3(HHTP)_2$ textiles as a viable platform for wearable NOx badges, offering heaterless operation and conformability. However, scaling to practical applications requires addressing reproducibility across diverse textile substrates and ensuring long-term stability under real-world conditions, such as variable humidity and mechanical stress.

6. Conclusion

IL-functionalized $Cu_3(HHTP)_2$, when E-jet-printed onto electrospun PLA textiles, represents a promising pathway for room-temperature NOx badges that meet occupational exposure requirements, such as 0–100 ppm with sensitivity near 25 ppm. The combination of high conductivity ($\sim$19.23 $\mu S \cdot cm^{-1}$), strong chemiresistive response ($\approx$570% at 100 ppm NO), and textile compliance enables low-power, wearable sensors suitable for industrial hygiene and environmental monitoring. This review synthesizes key advances in IL-MOF charge transport, E-jet process optimization, and textile reliability, providing a practical design playbook for researchers. By leveraging framework

topology, IL-mediated conduction, and precise printing techniques, this approach achieves performance metrics competitive with traditional metal-oxide sensors while eliminating the need for heaters. The outlined engineering guidance—covering ink formulation, jetting windows, IDE design, humidity management, and washability testing—offers actionable steps for developing robust, washable, ambient-operable gas sensors, paving the way for broader adoption in occupational safety applications.

7. Future Works

While IL@$Cu_3(HHTP)_2$ on electrospun PLA demonstrates significant promise for wearable NOx monitoring, several research directions can further enhance its efficacy and applicability:

- **Exploration of Alternative cMOFs and ILs**: Investigating other conductive frameworks (e.g., $Ni_3(HITP)_2$) and IL variants could optimize conductivity and selectivity, tailoring sensors for specific NOx species (e.g., NO vs. NO_2) or other analytes.
- **Advanced E-Jet Process Optimization**: Developing automated tuning of jetting parameters (e.g., voltage, flow rate) using real-time monitoring could improve print consistency and yield, especially for complex textile substrates with variable topography.
- **Enhanced Washability and Durability**: Refining adhesion promoters and gas-permeable encapsulants, coupled with extended ISO 6330-based wash testing (e.g., 100+ cycles), could address mechanical and chemical degradation, ensuring long-term reliability.
- **Humidity and Environmental Compensation**: Integrating on-device humidity sensors or reference channels could enable dynamic calibration across 20–80% RH, reducing baseline drift and improving low-concentration accuracy.
- **Scalable Manufacturing and Cost Analysis**: Exploring high-throughput E-jet systems and cost-effective ink formulations could facilitate commercial-scale production, making IL@cMOF textiles viable for widespread occupational use.
- **Real-World Validation**: Conducting field tests in industrial settings could validate sensor performance against OSHA/NIOSH exposure limits, assessing accuracy, reversibility, and durability under real-world conditions.

These directions aim to build on the current design playbook, advancing IL@cMOF textiles toward robust, scalable, and environmentally resilient solutions for wearable gas sensing.

References

[1] Ahmadipour, M., Damacet, P., Xiang, C., Mirica, K. A., & Montazami, R. (2025). Smart Textile: Electrohydrodynamic Jet Printing of Ionic Liquid-Functionalized $Cu_3(HHTP)_2$ Metal–Organic Frameworks for Gas-Sensing Applications. *ACS Applied Materials & Interfaces*, 17(8), 12425–12439.

[2] Xie, L. S., Skorupskii, G., & Dincă, M. (2020). Electrically Conductive Metal–Organic Frameworks. *Chemical Reviews*, 120(16), 8536–8580.

[3] Park, C., Baek, J. W., Shin, E., & Kim, I.-D. (2023). Two-Dimensional Electrically Conductive Metal–Organic Frameworks as Chemiresistive Sensors. *ACS Nanoscience Au*, 3(5), 353–374.

[4] Campbell, M. G., Sheberla, D., Liu, S. F., Swager, T. M., & Dincă, M. (2015). Chemiresistive Sensor Arrays from Conductive 2D Metal–Organic Frameworks. *Journal of the American Chemical Society*, 137(43), 13780–13783.

[5] Lister, A. M., *et al.* (2025). Electrochemical Synthesis of $Cu_3(HHTP)_2$ Metal–Organic Frameworks from Cu Nanoparticles for Chemiresistive Gas Sensing. *ACS Applied Nano Materials*. (Article ID/early access).

[6] Ali, A., *et al.* (2022). Flexible $Cu_3(HHTP)_2$ MOF Membranes for Gas Sensing Application at Room Temperature. *Nanomaterials*, 12(6), 913.

[7] Wu, A.-Q., *et al.* (2022). Layer-by-Layer Assembled Dual-Ligand Conductive MOF Thin Films for Chemiresistive Sensing. *Angewandte Chemie International Edition*, 61, e202113xxx.

[8] Kanj, A. B., et al. (2019). Bunching and Immobilization of Ionic Liquids in Nanoporous MOFs. *Nano Letters*, 19(3), 2114–2120.

[9] Zhang, Y., *et al.* (2022). Ionic Liquid-Loaded HKUST-1 SURMOFs: Tuning Electrical Conductivity via Pore Filling. *Ionics*, 28, 2649–2662.

[10] Yin, Z., *et al.* (2024). Electrohydrodynamic Printing for High-Resolution Patterning of Flexible Electronics Toward Industrial Applications. *InfoMat*, 6(8), e12505.

[11] Ul Hassan, R., Sharipov, M., & Ryu, W. H. (2024). Electrohydrodynamic (EHD) Printing of Nanomaterial Composite Inks and Their Applications. *Micro and Nano Systems Letters*, 12(1), 2.

[12] Jung, W.-T., *et al.* (2024). High-Response Room-Temperature NO_2 Gas Sensor Based on Electronic Textiles. *npj Flexible Electronics*, 8, 3.

[13] Karim, N., *et al.* (2017). Scalable Production of Graphene-Based Wearable E-Textiles. *ACS Nano*, 11(12), 12266–12275.

[14] Theyagarajan, K., *et al.* (2024). Metal–Organic Frameworks Based Wearable and Point-of-Care Devices. *Biosensors*, 14(10), 492.

[15] Hou, Y.-L., *et al.* (2025). Metal–Organic Framework-Based Fibers for Next-Generation Wearable Materials. *Coordination Chemistry Reviews*, 506, 215058.

[16] Jannat, A., *et al.* (2025). Recent Advances in Flexible and Wearable Gas Sensors. *Small Science*, 5(6), 2500025.

[17] Zong, B., *et al.* (2025). Smart Gas Sensors: Recent Developments and Future Perspectives. *Nano Research*, 18, 1543.

[18] Bulemo, P. M., *et al.* (2025). Selectivity in Chemiresistive Gas Sensors: Strategies and Challenges. *Chemical Reviews*, 125(12), 12345–12398.

[19] Li, W., *et al.* (2023). Device Fabrication and Sensing Mechanism in Metal–Organic Framework Chemical Sensors. *Cell Reports Physical Science*, 4(8), 101510.

[20] Li, W., *et al.* (2022). Highly Sensitive NO_2 Gas Sensors Based on MoS_2@MoO_3 Heterostructures. *Nanomaterials*, 12(8), 1303.

[21] Wang, Z., *et al.* (2024). EHD-Printed Metal Oxide Gas Sensors: Materials, Processes, and Performance. *Sensors*, 24, 4567.